FELIX

Multiparticle Production Structure in hh Collisions at 14 TeV

Alberto Giovannini and Roberto Ugoccioni
Dipartimento di Fisica Teorica, Università di Torino
and INFN, Sezione di Torino, via Giuria 1, 10125 Torino, Italy

1 Motivations of this study

The access to a new energy domain in high energy hh collisions at LHC demands to discuss the expected multiparticle production structure. We focus our attention to hh collisions at 14 TeV c.m. energy as requested by the FELIX programme. The study will be limited here to full phase space; it is the result of the analysis of the available experimental data at lower c.m. energies as well as of the most successful phenomenological models and QCD inspired Monte Carlo calculations.

2 What we learned from data at lower energies

The negative binomial (NB) behaviour reproduces data fairly well from the accelerator region up to 200 GeV c.m. energy [1, 2, 3]. The NB parameter k (which is linked to the dispersion D by the relation $k^{-1} = (D^2 - \bar{n})/\bar{n}^2$) decreases as the c.m. energy increases, while the average charged multiplicity $\bar{n}$ increases. This behaviour is compatible, in the PS-ISR energy range, with KNO scaling, as it makes $D^2/\bar{n}^2 = 1/k + 1/\bar{n}$ approximately constant with energy. It should be stressed that the parameter k controls also the correlation structure of multiparticle final states [4]:

$$\frac{1}{k} = \frac{1}{\bar{n}^2} \int C_2(y_1, y_2) dy_1 dy_2 \tag{1}$$

where $C_2(y_1, y_2)$ is the two-particle rapidity correlation function and the integral is over full phase space for the purpose of this paper. Therefore an increase of k^{-1} with c.m. energy signifies a strengthening of correlations among final particles. In addition, in view of the hierarchical correlation structure of the NB distribution (NBD) the behaviour of k^{-1} determines the correlations at any order. Thus the parameter k^{-1} turns out to be of fundamental relevance in our study.

Two facts are particularly interesting at c.m. energy above 200 GeV: a shoulder structure is clearly visible in the charged particles multiplicity distribution (MD), which violates the NB behaviour, and the ratio H_q of factorial moments over factorial cumulants of order q oscillate as a function of the order. We proceed as follows: we show first, following [5], that the observed shoulder structure, and the subsequent NB regularity violation, can be explained as the superposition of two types of events, here called "soft" and "semi-hard",

Table 1: Values of the parameters of eq. (2) fitted to UA5 data [7].

c.m. energy	α_0	$\bar{n}_1$	k_1	$\bar{n}_2$	k_2
200 GeV	0.93	19.9	7	42.2	79
546 GeV	0.75	24.0	7	47.6	14
900 GeV	0.72	26.9	7	57.9	13

which can be identified with events without mini-jets and with mini-jets, respectively [6]. It should be noticed that each contribution to the total MD is of NB type, *i.e.*, the total MD is given by:

$$P_n(\alpha_0; \bar{n}_1, k_1; \bar{n}_2, k_2) = \alpha_0 P_n^{\rm NB}(\bar{n}_1, k_1) + (1 - \alpha_0) P_n^{\rm NB}(\bar{n}_2, k_2) \tag{2}$$

where α_0 is energy dependent and corresponds to the fraction of soft events, the index 1 (2) denotes quantities referring to the soft (semi-hard) component, and

$$P_n^{\rm NB}(\bar{n}, k) = \frac{k(k+1)\cdots(k+n-1)}{n!} \frac{\bar{n}^n k^k}{(\bar{n}+k)^{n+k}} \tag{3}$$

is the NB distribution. In Table 1 we show the values of the parameters of the two distributions fitted to UA5 data at 200, 546 and 900 GeV c.m. energies. In Figure 1 the corresponding MD's (solid lines) are shown together with the breakdown in the two components (dotted lines). In Figure 2 the oscillations of H_q vs q are seen to be well described by the behaviour extracted from eq. (2).

These facts are relevant because they show at which level the NB regularity is really working above 200 GeV c.m. energy and that the shoulder effect in MD as well as H_q oscillations can be explained in hh collisions in terms of the same cause, *i.e.*, the superposition of soft and semi-hard contributions. A similar situation occurs in e^+e^- annihilation at LEP energy where both effects were observed and successfully interpreted as the superposition of events of different topology (different number of jets), and each sample of fixed topology was found to satisfy NB behaviour [8, 9].

Figure 1 shows also the results of Monte Carlo calculations, using Pythia [10] version 5.7 with multiple interactions turned on with variable impact parameter (corresponding to parameter MSTP(82) = 4; 5000 events were generated at each energy): the disagreement of these predictions with the data is rather evident.

Some conclusions can be drawn at this point:

1) for c.m. energies below 200 GeV, *i.e.*, in the region where the soft contribution is dominant, a single NBD describes data very well.

2) for c.m. energies above 200 GeV, *i.e.*, in the region where semi-hard contributions become more and more important two NBD's are needed in order to describe data and we propose to associate one of them to the soft component and the other to the semi-hard component. The relative weight of each component is given by the fits according to eq. (2) and was shown in Table 1.

In order to explore the new energy domain we stay with eq. (2) for several reasons:

a) QCD calculations are at present not yet ready to describe the final charged particles MD's and the H_q oscillations in the new region;

Table 2: Values of the parameters of eq. (2) at c.m. energy 14 TeV from the extrapolation described in the text.

parameter:	Scenario 1:	Scenario 2:
α_0	0.30	0.30
$\bar{n}_1$	39.5	39.5
k_1	7	7
$\bar{n}_2$	79	79
k_2	13	3
$\bar{n}$	67.2	67.2
k	7.3	2.46

b) Monte Carlo calculations (Pythia) give so far unsatisfactory results in the energy range available for hh collisions and their extrapolation to higher energy is expected to be questionable although indicative.

c) The successful presence of the NB regularity at a more fundamental level of investigation than usually done is clear, as was shown in this section, and its use as a tool to extrapolate to higher energies is therefore very valuable.

3 Extrapolation to the new energy domain

The first assumption concerns the energy dependence of the total average charged particle multiplicity, $\bar{n}$, which, following standard phenomenological fits [2] is taken equal to

$$\bar{n}(\sqrt{s}) = 3.01 - 0.474 \ln \sqrt{s} + 0.754 \ln^2 \sqrt{s} \tag{4}$$

Values from this, and from the other equations discussed in this section, at c.m. energy 14 TeV are given in Table 2. Notice that quantities without an index refer to the total MD, while the index 1 (2) refers to the soft (semi-hard) component.

Then, we assume for $\bar{n}_1$, the average charged particle multiplicity of the soft component, a logarithmic increase with the c.m. energy, as seen in all the data up to $\sqrt{s} = 900$ GeV:

$$\bar{n}_1(\sqrt{s}) = -5.54 + 4.72 \ln \sqrt{s} \tag{5}$$

Indications from Table 1, and from UA1 studies of mini-jets [11], suggest a useful relation for the average charged particle multiplicity of the semi-hard component:

$$\bar{n}_2(\sqrt{s}) \approx 2\bar{n}_1(\sqrt{s}) \tag{6}$$

which we propose to maintain at higher energy.

Since, from eq. (2), the above defined parameters are linked by the relation $\bar{n} = \alpha_0\bar{n}_1 + (1 - \alpha_0)\bar{n}_2$ it follows that we can determine the energy dependence of α_0:

$$\alpha_0 = \frac{\bar{n} - \bar{n}_2}{\bar{n}_1 - \bar{n}_2} = 2 - \frac{\bar{n}}{\bar{n}_1} \tag{7}$$

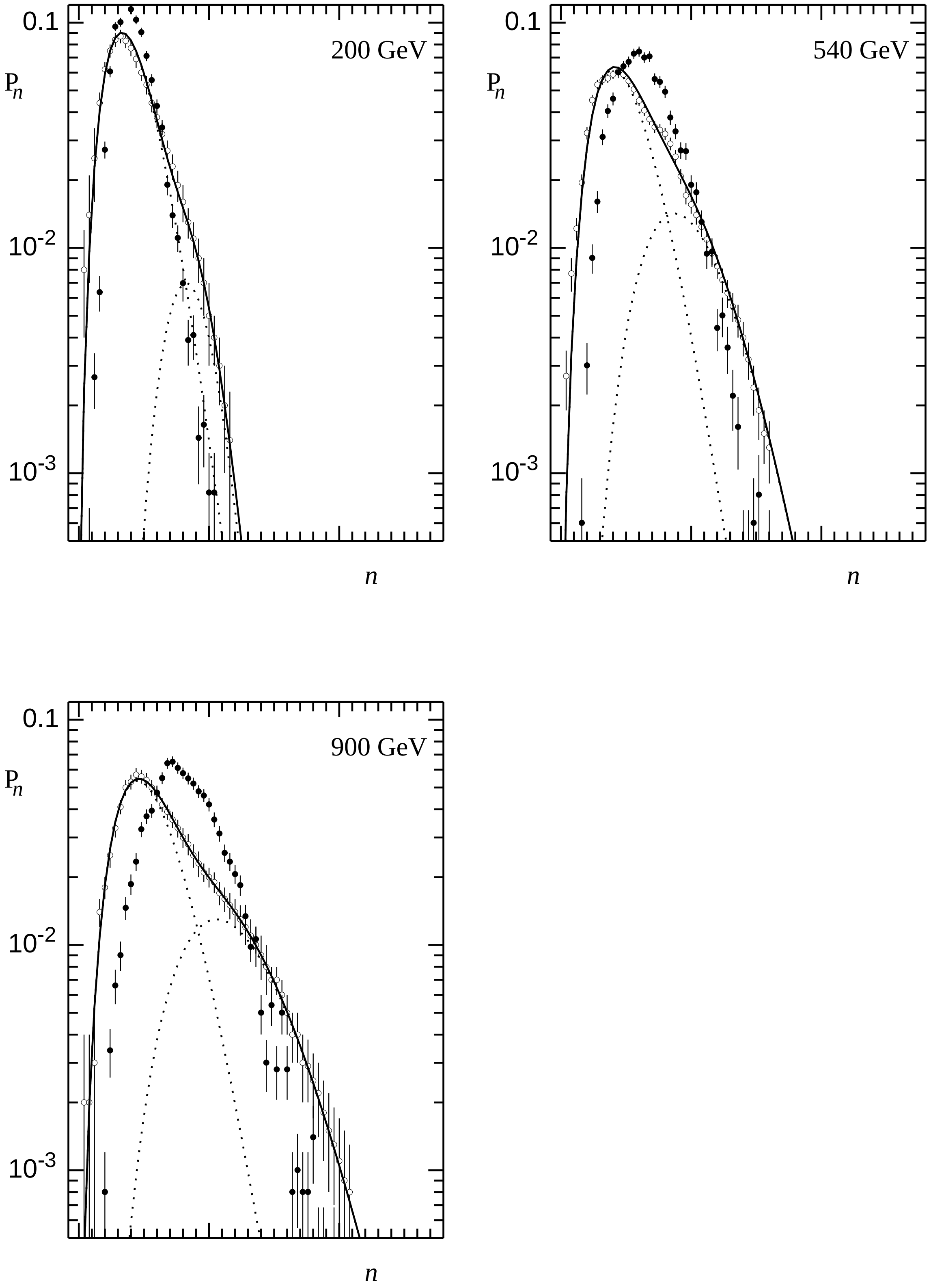

Figure 1: Charged particle multiplicity distributions at c.m. energies 200 GeV, 546 GeV and 900 GeV. Data (white dots) are from UA5 Collaboration; the solid line is the fit with eq. (2), whose components are given by the dashed lines. The solid dots show the result of Monte Carlo calculations (Pythia).

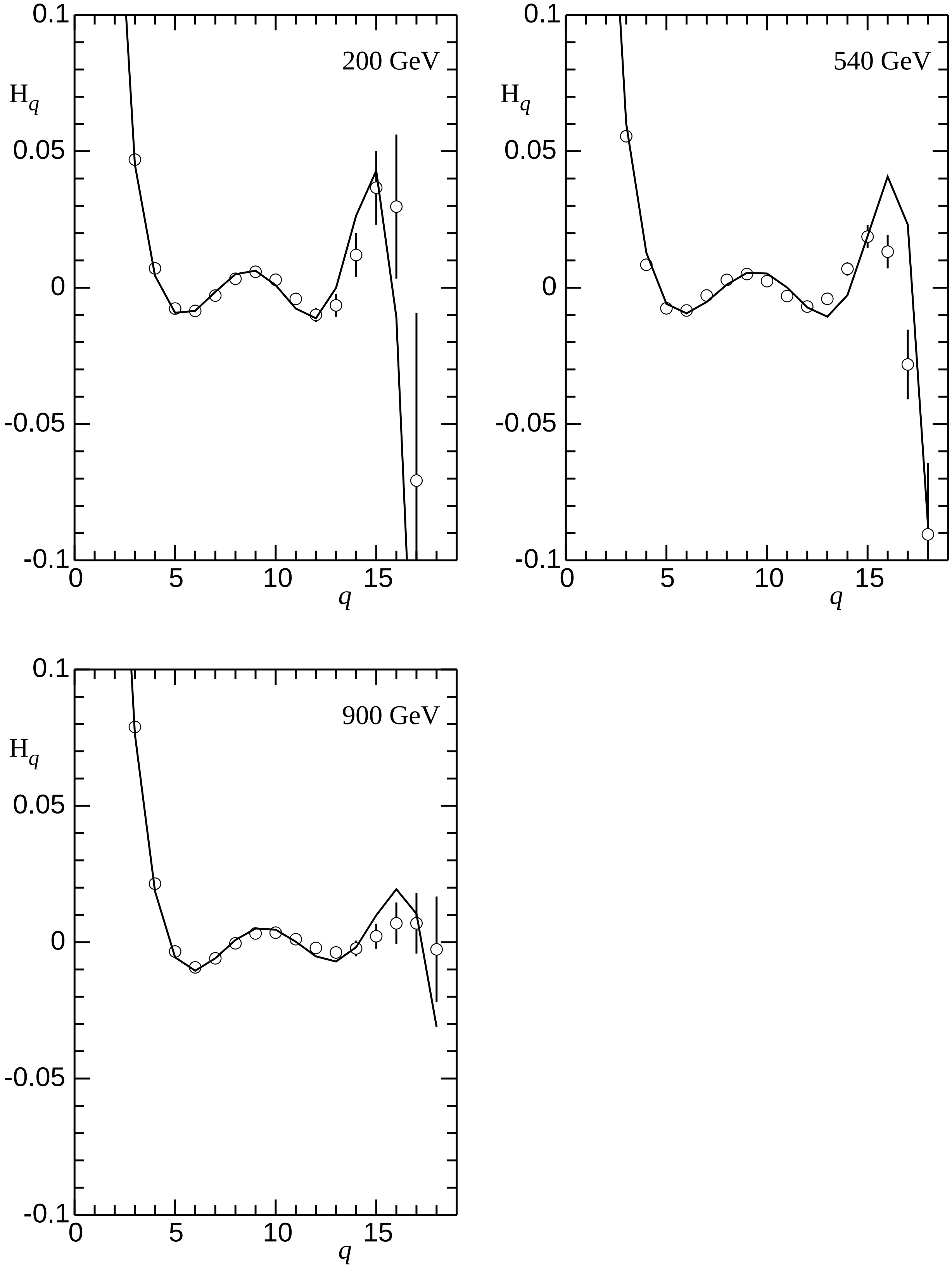

Figure 2: H_q vs q at c.m. energies 200 GeV, 546 GeV and 900 GeV. Data (dots) are from the MD's in Figure 1; the solid line is the prediction of the fit also shown in Figure 1.

The second problem is the energy dependence of k. Notice that at accelerator energies k coincides with k_1 (*i.e.*, only the soft component is present). Above 200 GeV c.m. energy the global distribution is not of NB type, so the parameter k is not defined. However, we can use the dispersion $D = \sqrt{\langle n^2 \rangle - \langle n \rangle}$, or, equivalently, the second factorial moment $F = \langle n(n-1) \rangle$, as

$$\frac{F}{\bar{n}^2} - 1 = \frac{D^2 - \bar{n}}{\bar{n}^2} = \frac{1}{k} \tag{8}$$

where the last equality is valid only when the MD is a NBD. The quantity on the left of eq. (8) is seen to increase, up to 900 GeV, approximately as:

$$\frac{D^2 - \bar{n}}{\bar{n}^2} = -0.0820 + 0.0512 \ln \sqrt{s} \tag{9}$$

Again from eq. (2) we see that the following relation holds:

$$F = \alpha_0 F_1 + (1 - \alpha_0) F_2 \tag{10}$$

Indications from Table 1 suggest that k_1 is constant at and above 200 GeV c.m. energy, and together with the small variation of $1/\bar{n}_1$ this implies that KNO [12] scaling is approximately satisfied by the soft component of the reaction.

We can therefore envision two scenarios for the variation of k_2 with energy:

Scenario 1: KNO scaling holds also for the semi-hard component. Because $1/\bar{n}_2$ is small, this implies that k_2 remains constant for c.m. energy $\sqrt{s} \geq 900$ GeV.

Scenario 2: $F/\bar{n}^2 - 1$ keeps growing logarithmically with c.m. energy, continuing the trend seen at lower energies, implying a strong KNO scaling violation above 200 GeV c.m. energy.

In comparing the two scenarios, it is very helpful to introduce the parameters of clan structure analysis [4], as has been done for all lower energy data (and for all reactions as well [13]). The average number of clans, $\bar{N}$, and the average number of particles per clan, $\bar{n}_c$, are linked to the NBD parameters through the following relations:

$$\bar{N}_i = k_i \ln(1 + \bar{n}_i/k_i) \qquad\qquad \bar{n}_{c,i} = \bar{n}_i/\bar{N}_i \tag{11}$$

with $i = 1, 2$. We can therefore define these parameters for the soft and the semi-hard components of the MD separately; globally however the shape is not of NB type, but since the two contributions are mutually exclusive, we can define the combinations:

$$\bar{N} = \alpha_0 \bar{N}_1 + (1 - \alpha_0) \bar{N}_2 \tag{12}$$

$$\bar{n}_c = \alpha_0 \bar{n}_{c,1} + (1 - \alpha_0) \bar{n}_{c,2} \tag{13}$$

Values for clan structure parameters at 14 TeV c.m. energy are given in Table 3.

The general situation implied by the two mentioned scenarios is summarized in Figure 4 for scenario 1 and Figure 5 for scenario 2, which show the behaviour of the NB parameter k_i (part a), of clan structure analysis parameters $\bar{N}_i$ and $\bar{n}_{c,i}$ (parts c and d) and of the KNO scaling parameter $D_i^2/\bar{n}_i^2$ (part b) for the soft and semi-hard components ($i = 1$ and 2 respectively). Since, according to our assumptions, the behaviour of

Table 3: Values of the parameters for clan structure analysis of eq. (2), at c.m. energy 14 TeV from the extrapolation described in the text.

parameter:	Scenario 1:	Scenario 2:
α_0	0.30	0.30
$\bar{N}_1$	13.3	13.3
$\bar{n}_{c,1}$	3.0	3.0
$\bar{N}_2$	25.4	9.92
$\bar{n}_{c,2}$	3.1	7.9
$\bar{N}$	21.5	11.0
$\bar{n}_c$	3.1	6.4

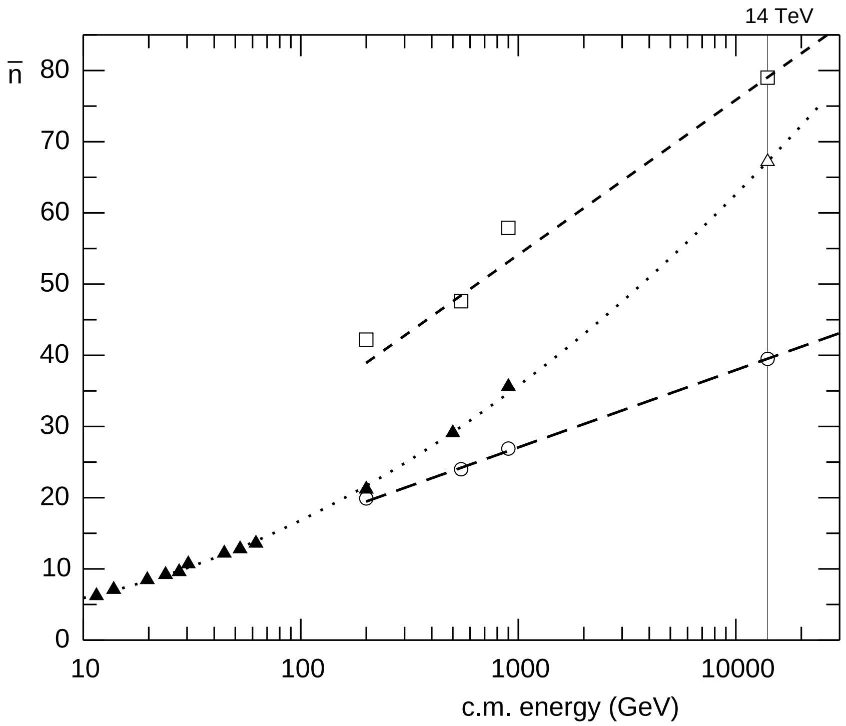

Figure 3: Average charged multiplicity vs c.m. energy. Full phase space data from accelerators, ISR and UA5 (filled triangles) are shown together with fits to the soft (open circles) and semi-hard (open squares) components. The lines show the extrapolation discussed in the text (long dashes, soft component; short dashes, semi-hard component; dots, total average charged multiplicity). The points at 14 TeV are all extrapolations.

the average charged multiplicity in the same in both scenarios, it is shown separately in Figure 3.

The differences between the two scenarios are, as already said, related to the different behaviour of $(D^2 - \bar{n})/\bar{n}^2$: in Figure 4a the constancy of k_1 (above 200 GeV c.m. energy) and of k_2 (above 900 GeV c.m. energy) implies that the variable is a decreasing function of the c.m. energy and equal to 0.163 at 14 TeV; in Figure 5a the requested linear increase of $(D^2 - \bar{n})/\bar{n}^2$ up to 0.4 at 14 TeV, together with the constancy of k_1, implies that $1/k_2$ increases also with energy, up to 0.33 at 14 TeV. The relevance of these different behaviours can be interpreted in terms of clan structure analysis.

In the first scenario, Figure 4, the average number of clans of both the soft and the semi-hard components increases with c.m. energy (the first being in general much smaller than the second, at 14 TeV 13.3 vs 25.4); the resulting weighted average number of clans is 21.6 at 14 TeV. It is interesting to remark that in all the above mentioned cases the average number of particles per clan grows logarithmically with energy and it is approximately the same at all energies, and it is 3.1 at 14 TeV. That the clan size is the same for the soft and the semi-hard component is the most striking result predicted by scenario 1.

In the second scenario, Figure 5, a different structure appears: the average number of clans of the soft component grows with energy as in the previous case and it is of course 13.3 at 14 TeV; on the contrary, the average number of clans of the semi-hard component is a decreasing function of the c.m. energy: it is 9.92 at 14 TeV. The crossing point of $\bar{N}_1$ and $\bar{N}_2$ is around 4 TeV. The total average number of clans also decreases with energy: at 14 TeV it is 11. In addition, the clan size of the semi-hard component is a steeply increasing function of the c.m. energy; it is equal to 7.9 at 14 TeV, a very large number compared to low energy results. The behaviour of $\bar{n}_{c,1}$ is of course the same as in scenario 1; consequently the weighted size of the two components at 14 TeV turns out to be 6.4. In conclusion, the average number of clans of the semi-hard component decreases with energy whereas their size is rapidly increasing.

The charged multiplicity distributions corresponding to the two scenarios are plotted in Figure 6 and 7. The parameters of the soft and semi-hard components are those indicated in Table 2. To the identical behaviour of the soft component in the two scenarios there corresponds a totally different behaviour of the semi-hard component and of course of the resulting total MD. In the same figures the charged particles MD predicted by Monte Carlo calculations (Pythia, with 10000 events, and with the same parameters as in section 2) are also shown: it is interesting to remark that these are incompatible with the results of scenario 1. On the contrary scenario 2 seems to show a trend similar to Pythia results, but the Monte Carlo gives a larger tail.

Finally, it should be added that it is not possible to give here predictions for the ratio H_q, as its oscillations with q depend very much on the truncation effect, *i.e.*, on the finite size of the experimental sample.

4 Conclusions

On KNO scaling behaviour:

The two proposed scenarios represent two extreme situations. In scenario 1, KNO scaling dominance is assumed, the result is that at 14 TeV $D^2/\bar{n}^2$ has the same value found in the PS-ISR region; in scenario 2, the KNO scaling violation observed by the

UA5 Collaboration is assumed to increase, consequently $D^2/\bar{n}^2$ reaches the value ≈ 0.42 to be compared with 0.2 in the PS-ISR region.

On the correlation structure:

In scenario 1 correlations of the soft and semi-hard components do not change with energy, whereas those of the total MD decrease with energy from a maximum reached at $\approx$ 900 GeV c.m. energy. In scenario 2 correlations of the semi-hard component of the total MD are much stronger than those of the soft component and are expected to grow with energy.

On clan structure analysis:

In scenario 1 the clan size is the same in both components (and of course in the total MD) and it is slowly growing with energy. The average number of clans on the contrary is much larger in the semi-hard than in the soft component although its general trend is the same. In scenario 2 the clan size in the semi-hard component (and in the total MD) is rapidly increasing with c.m. energy and results much larger than in the soft component. On the contrary the average number of clans decreases with energy and becomes at high energy smaller than in the soft component and approximately equal to that of the total MD.

On multiplicity distributions:

In scenario 1 the maximum of the MD is at ≈ 70 particles, whereas in scenario 2 it is ≈ 35; correspondingly, since the total average multiplicity is the same in both scenarios, the tail of the MD is much higher in scenario 2 than in scenario 1. It should also be noticed that the semi-hard component is negligible at low multiplicity in scenario 1, but not in scenario 2 where it is actually larger than the soft one. Finally, QCD inspired Monte Carlo calculations predict a MD which is closer (from below) to scenario 1 in the low multiplicity region but closer (from above) to scenario 2 in the high multiplicity tail.

References

1. A. Giovannini, Il Nuovo Cimento 10A (1972) 713; A. Giovannini, Lett. al Nuovo Cimento 6 (1973) 514; A. Giovannini, P. Antich, E. Calligarich, G. Cecchet, R. Dolfini, F. Impellizzeri, S. Ratti, Il Nuovo Cimento 24A (1974) 421; M. Garetto, A. Giovannini, E. Calligarich, G. Cecchet, R. Dolfini, S. Ratti, Il Nuovo Cimento 38A (1977) 38.
2. G. Giacomelli and M. Jacob, Physics Reports 55 (1979) 1 and references quoted therein.
3. G.J. Alner et al., UA5 Collaboration, Physics Reports 154 (1987) 247.
4. A. Giovannini and L. Van Hove, Z. Phys. C 30 (1986) 391.
5. C. Fuglesang, in Multiparticle Dynamics: Festschrift for Léon Van Hove (La Thuile, Italy, 1989) eds. A. Giovannini and W. Kittel: World Scientific, Singapore, 1990, p. 193.
6. A. Giovannini and R. Ugoccioni, to appear in the Proceedings of the QCD Euro-conference 97 (Montpellier, France, July 3–9, 1997).
7. R.E. Ansorge et al., UA5 Collaboration, Z. Phys. C 43 (1989) 357.
8. A. Giovannini, S. Lupia and R. Ugoccioni, Phys. Lett. B 374 (1996) 231.
9. A. Giovannini, S. Lupia and R. Ugoccioni, Phys. Lett. B 388 (1996) 639.
10. T. Sjöstrand and M. Bengstsson, Computer Physics Commun. 82 (1994) 74.
11. C. Albajar et al., UA1 Collaboration, Nucl. Phys. B 309 (1988) 405
12. Z. Koba, H.B. Nielsen and P. Olesen, Nucl. Phys. B 40 (1972) 317.
13. A. Giovannini, to be published in Proceedings of the XXVI International Symposium on Multiparticle Dynamics (Faro, Portugal, September 1–5, 1996).

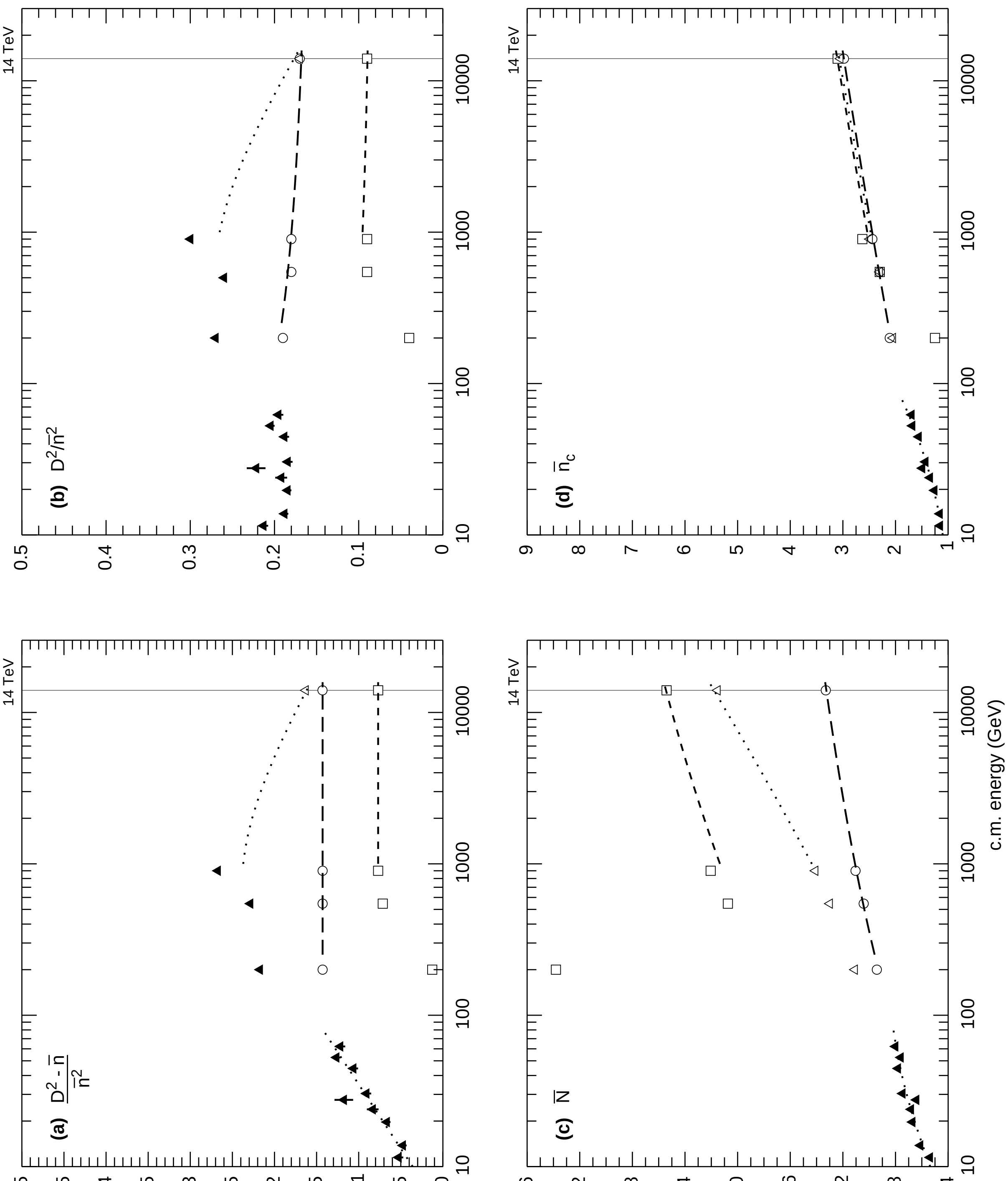

Figure 4: Behaviour of parameters of the MD in scenario 1 (KNO scaling dominance): NB parameter k (**a**), of clan structure analysis parameters $\bar{N}$ (**c**) and $\bar{n}_c$ (**d**) and of the KNO scaling parameter $D^2/\bar{n}^2$ (**b**). Full phase space data from accelerators, ISR and UA5 (filled triangles) are shown together with fits to the soft (open circles) and semi-hard (open squares) components. Open triangles show the weighted sum of the components. The lines show the extrapolation discussed in the text (long dashes, soft component; short dashes, semi-hard component; dots, total MD). The points at 14 TeV are all extrapolations.

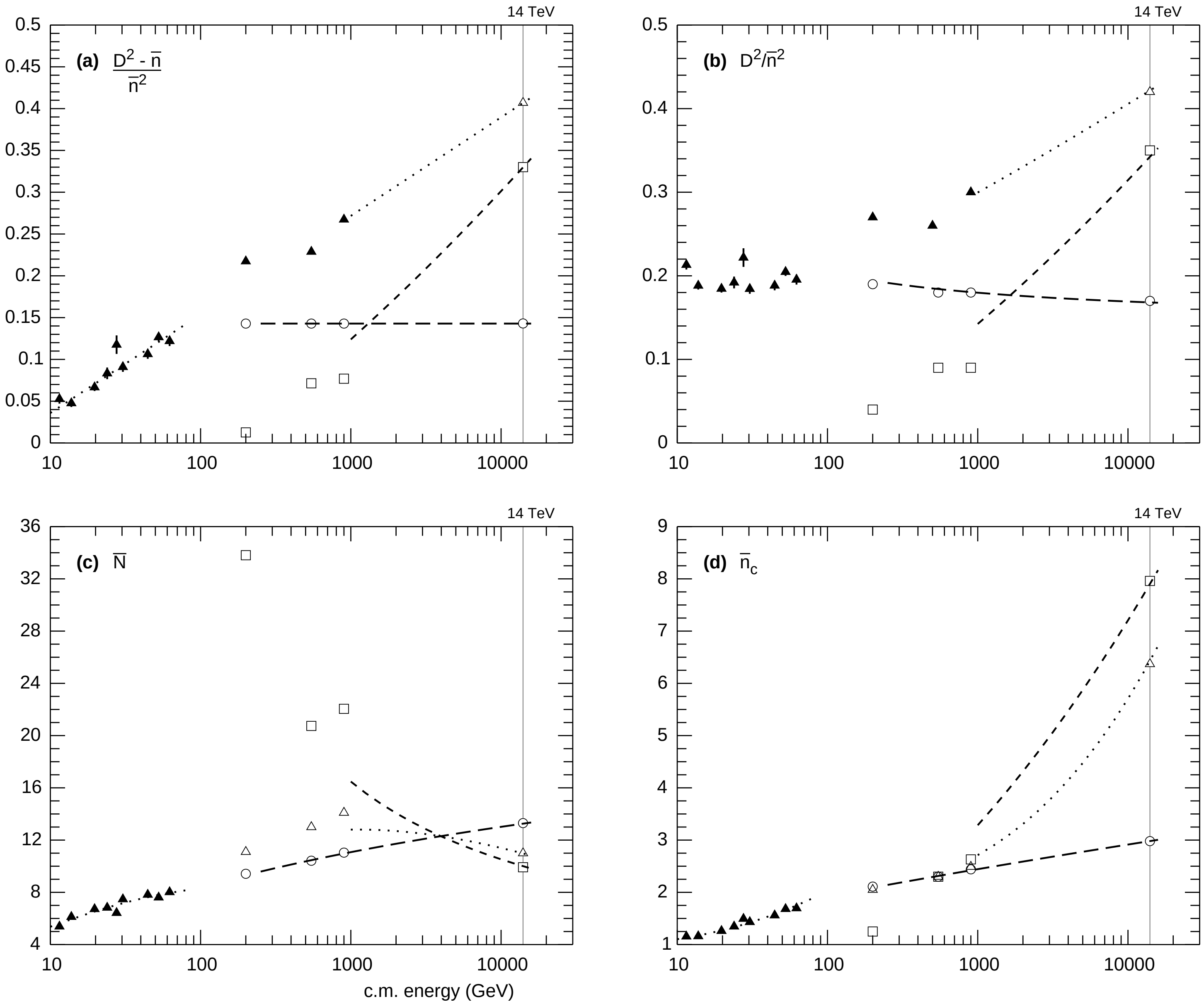

Figure 5: Same as Figure 4 but for scenario 2 (KNO scaling violation).

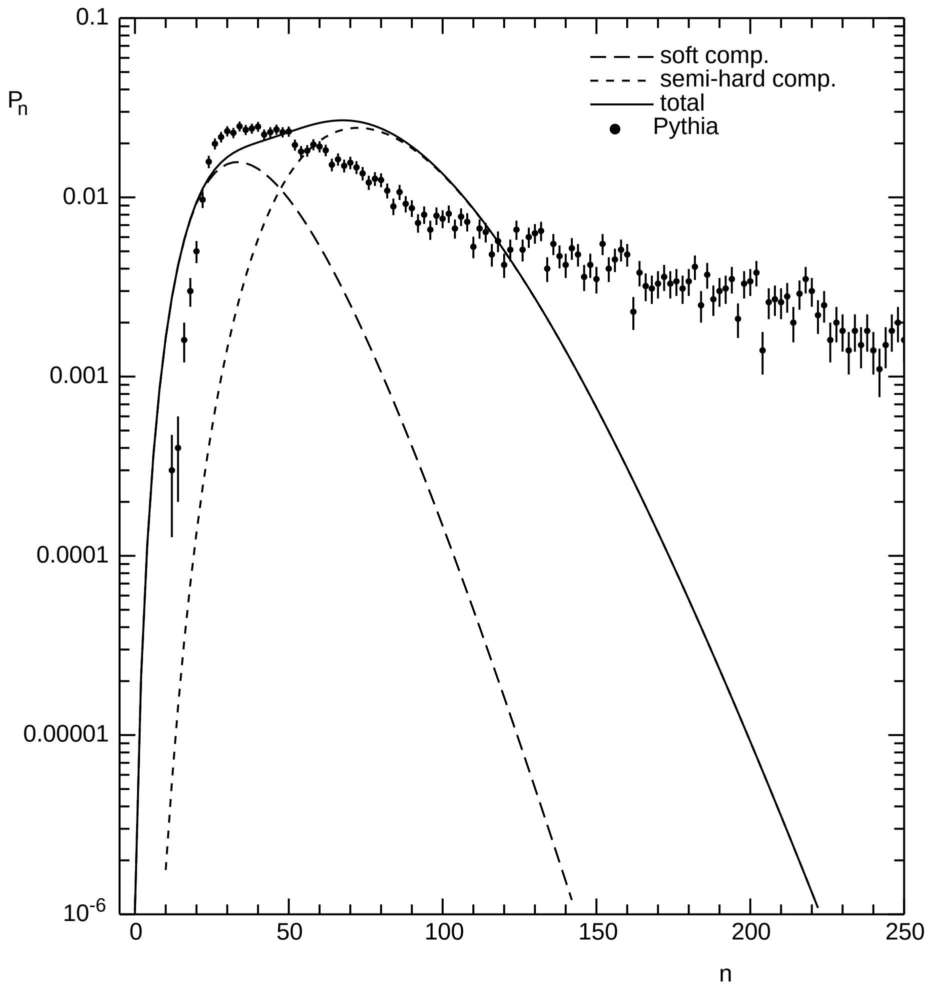

Figure 6: Charged particle multiplicity distributions at 14 TeV for scenario 1 (KNO scaling dominance). The long- and short- dashed lines represent the soft and the semi-hard component respectively, the solid line represents the total MD. Dots are Pythia Monte Carlo predictions.

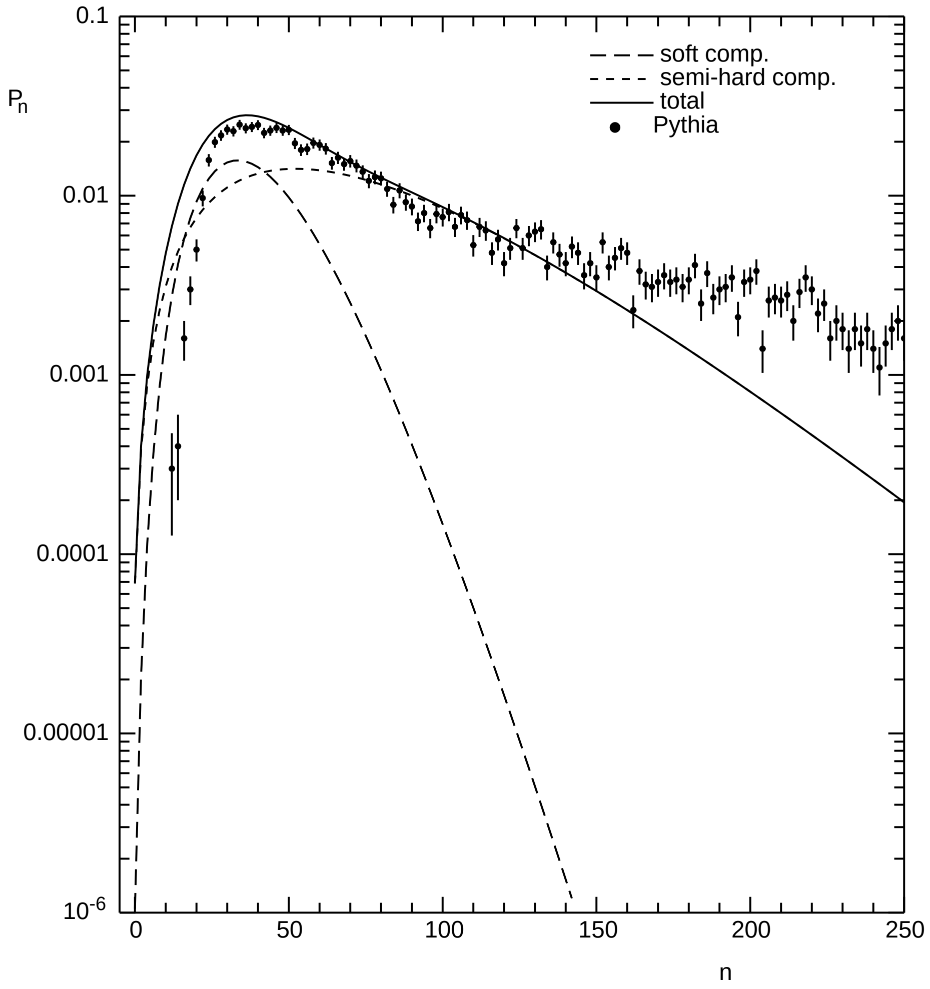

Figure 7: Same as Figure 6 but for scenario 2 (KNO scaling violation).